Internal Rotation of 1-Aryl-3,3-dialkyltriazenes. Comparison of Semiempirical Molecular Orbital Calculations with Far-Infrared, Raman, and NMR Spectroscopic Results

J.-C. Panitz, T. Lippert, and A. Wokaun*

Physikalische Chemie II, Universität Bayreuth, D-95440 Bayreuth, Germany

Received: March 24, 1994; In Final Form: June 10, 1994®

Internal rotation in 1-(3-carboxyphenyl)-3,3-dialkyltriazenes has been investigated using PM3 and AM1 semiempirical molecular orbital techniques; methyl, ethyl, and isopropyl groups have been considered for the alkyl substituents. The purpose of this study is to establish a model for internal rotation about the N2–N3 axis in the mentioned class of compounds. Potential energy curves are analyzed with a truncated Fourier series approach, and a qualitative explanation for the shape of the curve is provided. Results obtained by vibrational and NMR spectroscopy are used to judge the reliability of the semiempirical methods used for the present problem. Agreement between experimental and calculated results is satisfactory for the PM3 parametrization. In contrast, when the AM1 method is used, an artifact in the potential energy curve of internal rotation about the N2–N3 axis is observed. The reason for this difference in performance of the two parametrizations used is discussed.

Introduction

Recently a novel application of 1-aryl-3,3-dialkyltriazenes has been demonstrated. When these compounds are added into polymer matrices, they act as efficient promoters of laser-induced polymer ablation. Several studies were carried out in order to establish the mechanisms which are important in the ablation of doped polymers.[1] Evidence is accumulating that photochemical extrusion of nitrogen from the dopant molecules by a radical pathway[2,3] leads to the observed enhancement of polymer ablation, particularly in the low fluence regime. Therefore, extensive studies have been aimed at elucidating the properties of the triazene chromophore. The N2–N3 bond of the triazene moiety possesses a considerable partial double bond character. The reason for this charge delocalization may be represented in terms of the two mesomeric structures[4] shown in Scheme 1. The second mesomeric structure, II, features a double bond between nitrogen centers N2 and N3. Any contribution of this formal resonance structure to the actual electron density distribution will result in a 1,3-dipolar character of the triazene moiety. The increased bond order between N2 and N3 leads to a high barrier for internal rotation around this axis. Activation energies of internal rotation for the latter degree of freedom have been derived for several triazenes by NMR[5] and Raman/mass spectrometric studies.[6]

In the mentioned investigations,[5,6] the effects of aryl and alkyl substituents on the hindered rotation have been studied. From dynamic NMR measurements, only the overall height of potential energy barriers to internal rotation can be assessed. To obtain more insight into the motions involved in this torsional degree of freedom and into the shape of the associated potential energy function, we decided to calculate the potential energy surface related to the internal motion about the N2–N3 axis. With the aim of establishing a transferable model for the latter degree of freedom in 1-aryl-3,3-dialkyltriazenes, the compound 1-(3-carboxyphenyl)-3,3-dimethyltriazene was chosen as a representative example. The internal rotation of one of the methyl groups attached to center N3 was considered in addition in the present calculation.

Both AM1 and PM3 parametrizations have been employed in our semiempirical molecular orbital calculations. These two methods had been successfully applied to the class of compounds under study in our earlier investigation.[7] An early calculation of the height of the barrier to rotation around the N2–N3 axis in 1-(3-carboxyphenyl)-3,3-dimethyltriazene had been performed by Ramos and Pereira[8] using the semiempirical MNDO method. As a consequence of the simplifying assumptions that had to be adopted, the barrier heights reported in ref 8 turned out to be not directly transferable to our present application. The validity of the semiempirical models used was tested by a comparison with relevant experimental parameters from spectroscopic measurements. To establish trends within a series of structurally related compounds, two triazene derivatives carrying different alkyl substituents at N3, i.e., 1-(3-carboxyphenyl)-3,3-diethyl-triazene and 1-(3-carboxyphenyl)-3,3-diisopropyltriazene, have been included in the investigation.

SCHEME 1: Mesomeric Structures of (3-Carboxyphenyl)-3,3-dimethyltriazene

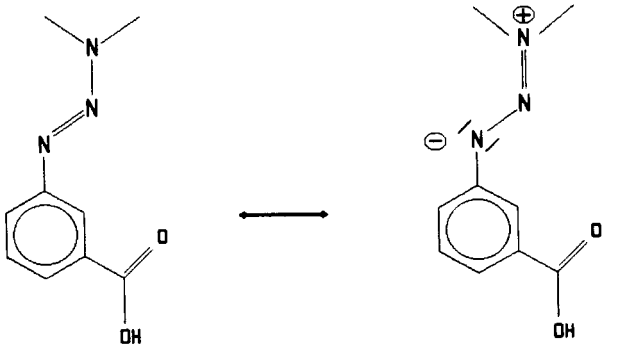

I II

Experimental Section

Preparation of Investigated Compounds. 1-(3-Carboxyphenyl)-3,3-dimethyltriazene (**1**), 1-(3-carboxyphenyl)-3,3-diethyltriazene (**2**), and 1-(3-carboxyphenyl)-3,3-diisopropyltriazene (**3**) were prepared according to the procedure described in ref 5.

Raman and Far-Infrared Spectroscopy. Raman spectra were acquired on a Bruker IFS 55 instrument equipped with a FT-Raman accessory (FRA 106). A diode-pumped Nd:YAG laser was used for excitation of the Raman spectra, with average power at the sample amounting to 15 mW. The scattered light was collected in a backscattering geometry. 256 scans were acquired at a resolution of 1 cm^{-1}. Far infrared spectra were run on a Bruker IFS 120 FTIR spectrometer in the wavelength range from 100 to 700 cm^{-1}; resolution was set to 1 cm^{-1}. 200 scans were

* To whom correspondence should be addressed.

® Abstract published in *Advance ACS Abstracts,* August 1, 1994.

0022-3654/94/2098-8817$04.50/0

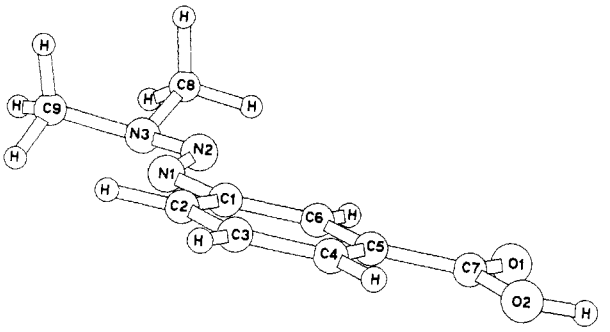

Figure 1. Molecular geometry of 1-(3-carboxyphenyl)-3,3-dimethyltriazene calculated under the PM3 parametrization. Labels refer to text and Tables 1 and 2 where some relevant bond lengths and bond angles are given.

coadded for each spectrum. The spectra were recorded from pellets consisting of 5 wt % of the triazene embedded in polyethylene (Aldrich, spectroscopic grade).

NMR Spectroscopy. NMR spectra were recorded for solutions of compound **1** in methanol-d_4 on a 300 MHz spectrometer (Bruker, Model AC300) equipped with a variable-temperature unit (Bruker, Model BVT 1000) in the temperature range 263–323 K. At low temperature, the signals due to the methyl protons consisted of a doublet, with a chemical shift difference $\Delta\nu = 102$ Hz. Coalescence of the doublet occurred at $T = 284$ K; at higher temperatures, a singlet was observed for the methyl proton resonances. As described in ref 5, parameters characterizing the exchange of the methyl groups by internal rotation were derived according to the line width method and are included in Table 4 below.

Quantum Chemical Calculations

Semiempirical molecular orbital calculations were carried out on a DECstation 5000/120 (Digital Equipment Corp., Nashua, NH). The program package SCAMP4.30[9] was used, which is based on MOPAC[10] and AMPAC[11] programs but offers some additional features. Generation of input files and processing of output files was conveniently handled with the aid of the graphical editor program SHOWMOLE.[12] AM1[13] and PM3[14] parametrizations were used for the calculations. A previous study[7] had shown that these methods provide an excellent representation of the molecular geometry of triazene compounds; this was tested by a comparison with the known X-ray structure of 3,3-dimethyl-1-(4-cyanophenyl)triazene.[15]

Calculations were performed without imposing any geometry or symmetry restrictions; all geometric parameters were allowed to vary during energy minimization. For instance, no predefined parameters for idealized methyl groups have been used. Molecular geometry was optimized in a two-step process. To verify that the structure resulting from this calculation did indeed represent a stationary point on the surface energy surface, the eigenvalues of vibration, rotation, and translation were calculated and found to have positive signs as required.[16]

The mentioned stationary point corresponding to the minimum energy conformation of the electronic ground state was used as a starting point for subsequent calculations. For compound **1**, a potential surface related to two degrees of freedom was calculated, i.e., internal rotation of the C8 methyl group around the N3–C8 axis, and internal rotation about the N2–N3 axis (cf. Figure 1). The energy surface was mapped by defining a value for the first of the two dihedral angles of interest, while incrementing the second one in steps of 10°. After calculation of 31 points (AM1) or 36 points (PM3), the fixed variable was increased by 10°. This process was repeated until potential surfaces consisting of 31 × 31 points (AM1), and 36 × 36 points (PM3) had been obtained.

TABLE 1: Bond Lengths, Bond Angles, and Dihedral Angles in the Triazene Group

	1		2		3	
	AM1	PM3	AM1	PM3	AM1	PM3
			Bond Lengths			
C1–N1	142.9	144.6	143.0	144.6	142.9	144.5
N1–N2	124.6	123.7	124.7	123.9	124.9	124.2
N2–N3	133.6	138.1	133.5	137.3	133.0	136.3
N3–C8	146.0	148.9	147.1	149.8	148.3	151.6
N3–C9	145.8	148.8	146.6	149.7	147.8	151.3
			Bond Angles			
C2–C1–N1	116.3	115.4	116.4	116.0	116.5	115.7
C6–C1–N1	124.6	124.1	124.7	123.4	124.6	123.9
C1–N1–N2	119.0	119.5	118.8	119.0	118.5	119.0
N1–N2–N3	119.7	117.3	120.2	117.6	121.0	118.4
N2–N3–C8	115.5	112.5	114.7	113.2	112.9	111.7
N2–N3–C9	124.2	121.1	124.5	122.7	123.2	121.8
C8–N3–C9	113.5	113.1	115.4	116.1	120.6	121.6
			Dihedral Angles			
C1–N1–N2–N3	172.7	174.7	172.5	175.3	173.4	175.9
N1–N2–N3–C8	158.3	161.6	161.3	168.1	165.7	172.6
N1–N2–N3–C9	9.3	23.1	8.2	20.7	6.0	17.0

TABLE 2: Selected Electronic Properties Calculated with AM1 and PM3

	1		2		3	
	AM1	PM3	AM1	PM3	AM1	PM3
			Heats of Formation/kJ mol^{-1}			
	10.9	−50.6	−41.8	−101.2	−27.5	−133.1
			Ionization Potential/eV			
	8.968	9.255	8.934	9.160	8.961	9.010
			Partial Charges on the Nitrogen Centers/e			
N1	−0.196	−0.107	−0.198	−0.122	−0.213	−0.147
N2	0.051	−0.030	0.051	−0.014	0.057	−0.011
N3	−0.233	0.000	−0.231	−0.015	−0.233	−0.008
			Bond Orders in the Triazeno Group			
N1=N2	1.752	1.821	1.744	1.805	1.725	1.775
N2–N3	1.117	1.088	1.122	1.105	1.140	1.138

In addition, the potential energy curve for internal rotation about the N2–N3 axis in compounds **2** and **3** was calculated in steps of 10°.

Results and Discussion

Molecular Geometry and Ground-State Properties. The molecular geometry of compound **1** is depicted in Figure 1, along with the labels of the atoms to be used throughout the text. Selected results for the geometric and electronic properties of the investigated compounds that are relevant for the subsequent discussion, are given in Tables 1 and 2. Differences between the bond lengths, bond angles, and dihedral angles calculated using the AM1 parametrization and those calculated by the PM3 parametrization are typically smaller than 3 pm or 3°, respectively.

However, there are marked differences in the calculated partial charges on the nitrogen centers of the triazene functional group. As mentioned in the Introduction, experimental evidence[5-7] clearly shows that the N2–N3 bond has partial double bond character and that there is a dipolar charge distribution within the triazene moiety, as represented in the formal mesomeric resonance structure II of Scheme 1. From an inspection of Table 2, it is evident that the AM1 model fails to reproduce this dipolar charge distribution. In the PM3 parametrization, the partial charge is about $-0.12e_0$ at the nitrogen center N1 and close to zero at nitrogen N3. However, one has to take into account the fact that the two alkyl substituents at N3 transfer a charge of about $-0.08e_0$ to nitrogen center N3,[7] such that the unsubstituted nitrogen atom would be positively charged by the same amount. Thus we find that PM3 does provide a more appropriate description of the dipolar character of the triazeno group, as compared to AM1.

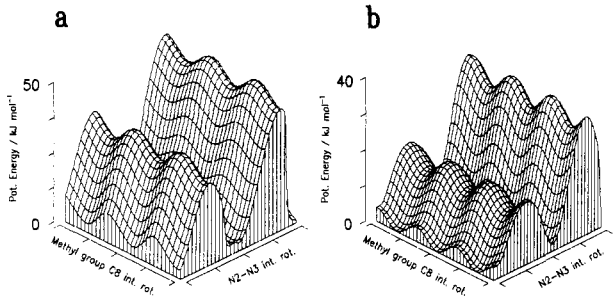

Figure 2. Potential energy surfaces for compound **1** calculated with (a) AM1 (31 × 31 points), and (b) PM3 (36 × 36 points). Note the asymmetry of the N2–N3 torsional potential calculated with AM1 and the steep descents from the maxima to the minima.

Potential Energy Surfaces. The surfaces describing the potential energy of internal rotations for compound **1** are compared in Figure 2 for the AM1 (a) and PM3 (b) parametrizations. In both cases, the internal rotation of the methyl group, with its 3-fold symmetry and the associated low energy, and the high barrier torsional motion about the N2–N3 axis are evident. For a more quantitative comparison, we refer to the truncated Fourier series analysis of the profiles, to be discussed in more detail below. The values of the coefficients obtained by least-squares analysis of sections through the calculated energy surfaces are listed in Tables 3 and 4.

The potential energy curve of methyl group rotation is not significantly dependent on the semiempirical model used (cf. Table 3). In contrast, it is obvious from an inspection of the potential energy surfaces that the N2–N3 torsion is modeled very differently in AM1, as compared to the PM3 model. In addition, the AM1 potential energy surface contains a peculiar discontinuity concerning the N2–N3 torsional degree of freedom, which will be discussed in detail below.

Analysis of Methyl Group Internal Rotation. The periodic potential energy function V governing the internal rotation of symmetric groups in molecules is best represented in terms of a Fourier series:[17]

$$V(\tau) = \sum_{i=1}^{\infty} \frac{V_i}{2}(1 - \cos(i\tau)) \qquad (1)$$

This approach has been used for both types of internal motion under discussion. For internal rotation of a methyl group, only the terms $i = 3n$ ($n = 1, 2, 3, \ldots$) in eq 1 are nonzero due to the C_{3v} symmetry of the methyl group. Often, the relation $|V_3| > |V_6| \gg |V_9|$ is found to hold,[17] such that only the 3-fold and sixfold terms of eq 1 have to be taken into account. Therefore, the potential energy function of methyl group internal rotation is expressed as

$$V(\tau) = \frac{V_3}{2}(1 - \cos 3\tau) + \frac{V_6}{2}(1 - \cos 6\tau) \qquad (2)$$

V_3 and V_6 are obtained by a least-squares fit of eq 2 to the calculated energy cross sections. Results for compound **1** are given in Table 3.

Internal rotation of a methyl group in the single particle approximation[18] can be described by a one-dimensional Schrödinger equation using the Hamilton operator

TABLE 3: Calculated Potential Energy Parameters and Energy Levels for the Internal Rotation of the Methyl Group C8 of Compound 1[a]

Potential Energy Parameters

V_i/kJ mol^{-1}	V_3	V_6
AM1	4.15	−0.10
PM3	3.70	−0.02

Calculated Energy Levels/cm^{-1}

label	0_a	1_e	2_e	$3_{a'}$	$3_{a''}$
AM1	59.24	59.26	170.96	171.40	264.02
PM3	56.55	56.58	162.47	163.26	247.10
	4_e	5_e	$6_{a'}$	$6_{a''}$	7_e
AM1	269.13	335.66	364.62	385.95	433.56
PM3	254.81	313.11	349.72	363.83	418.01

Comparison of Calculated with Experimental Transition Energies/cm^{-1}

transition	$3_{a''}$–0_a	2_e–1_e
AM1/LS[b]	112.16	111.70
PM3/LS[b]	106.71	105.89
AM1/NCA[b]	107.56	
PM3/NCA[b]	103.26	
FIR	257.7	303.8
Raman	281.7	306.8

[a] Transition energies deduced from potential energy curves are compared with values obtained by a normal coordinate analysis performed with SCAMP4.30 and with experimental data recorded with Raman and FIR spectroscopy. [b] LS: Calculated with potential energy parameters derived from least-squares analysis; NCA, SCAMP4.30 normal-coordinate analysis.

TABLE 4: Contributions to the Internal Rotation Potential Energy of the N2–N3 degree of Freedom As Obtained by a Least-Squares Fit to the Calculated Data[a]

	1		**2**		**3**	
V_i/kJ mol^{-1}	AM1	PM3	AM1	PM3	AM1	PM3
			Six-Parameter Fit			
V_1	−2.10 [1.27]	0.94 [0.05]	1.86 [0.93]	2.95 [0.11]	−1.14 [1.41]	5.94 [0.61]
V_2	35.73 [1.27]	20.40 [0.05]	36.53 [0.93]	24.91 [0.11]	39.35 [1.41]	35.89 [0.61]
V_3	−0.53 [1.27]	−0.74 [0.05]	−1.24 [0.93]	−1.80 [0.11]	1.00 [1.41]	−3.67 [0.61]
V_4	−1.46 [1.27]	0.97 [0.05]	−4.64 [0.93]	−0.02 [0.11]	−4.50 [1.41]	−2.97 [0.61]
V_1*	5.88 [1.63]	−6.55 [0.07]	4.14 [1.20]	−7.02 [0.11]	3.82 [1.81]	−5.32 [0.78]
V_2*	−3.43 [1.63]	0.04 [0.07]	−0.53 [1.20]	1.59 [0.11]	−2.22 [1.81]	2.07 [0.78]
			Three-Parameter Fit			
V_2	34.68 [1.13]	20.49 [0.04]	36.78 [0.68]	25.37 [0.17]	39.30 [1.09]	26.78 [0.73]
V_4	−2.51 [1.13]	1.05 [0.04]	−4.40 [0.68]	0.42 [0.17]	−4.57 [1.09]	−2.05 [0.73]
V_1*	5.88 [1.89]	−6.55 [0.07]	4.14 [1.14]	−7.01 [0.29]	3.82 [1.81]	−5.31 [1.21]
			Experimental Data[b]			
ΔG^*/kJ mol^{-1}		55.9 ± 2.8		57.5 ± 2.9		58.6 ± 2.9
E_a/kJ mol^{-1}		50.8 ± 2.5		45.8 ± 1.8		53.4 ± 1.8
$\tilde{\nu}$/cm^{-1}		192.1		193.0		194.5

[a] A comparison with experimentally obtained data is given. [b] NMR derived data for compounds **2** and **3** are taken from ref 5. Vibrational data are obtained with FT Raman spectroscopy.

$$\hat{H} = -B\frac{\partial^2}{\partial\tau^2} + V(\tau) \qquad (3)$$

where $B = h^2/8\pi^2 I_{CH_3}$ is the rotational constant of the methyl group, and $V(\tau)$ represents the potential energy operator defined in eq 2. Using this Hamiltonian the calculation of the eigenvalues and the eigenfunctions is a straightforward procedure, once the potential parameters are known.[19]

In case of a low barrier to internal rotation, a basis set of free rotor functions is used:

$$\Psi_{J,\sigma}(\tau) = \sqrt{\frac{1}{2\pi}}\sum_{-\infty}^{+\infty} c_{m\sigma}\exp\{i(m+\sigma)\tau\} \qquad (4)$$

Here the index J numbers the energy levels of the hindered rotor, whereas the label σ identifies the symmetry species of the wave function. It is well-known that the energy levels of hindered internal rotation of a CH_3 group are 3-fold degenerate in case of an infinitely high barrier.[20] For finite barriers, this degeneracy is partially lifted. The value $\sigma = 0$ corresponds to the wave function $\Psi_{J,A}$ of the totally symmetric symmetry species A, whereas $\sigma = \pm 1$ corresponds to the 2-fold degenerate wavefunctions of symmetry species E, labeled $\Psi_{J,E}$.

After setting up the Hamiltonian matrices, a Jacobi diagonalization routine is used to obtain the eigenvalues and eigenvectors, e.g., the coefficients associated with each wavefunction of the basis set. The size of the Hamiltonian matrix was chosen sufficiently large such that the 20 lowest eigenvalues no longer responded to an extension of the basis set.

The results of the least-squares fit of the calculated potential energy for the rotation of methyl group C8 of compound **1** are listed in Table 3, together with the results of the Jacobi diagonalization. Also included are the torsional frequencies of the methyl group of **1**, as calculated by a normal coordinate analysis performed with SCAMP4.30. In addition, the frequencies observed by Raman and FIR spectroscopy and assigned to methyl group internal rotation are presented (cf. discussion below).

Whereas the results obtained by the diagonalization procedure compare well with the torsional frequency of the methyl group derived from the SCAMP4.30 normal-coordinate analysis, there are considerable differences between the calculated and experimentally obtained values. Fabian[21] has reported on a similar observation, i.e., that the barrier heights calculated within the AM1 parametrization are often too small as compared to experimentally derived data. In the present case, use of the PM3 parametrization yields no improvement.

Analysis of Torsion about the N2–N3 Axis. For the potential energy curve characterizing the torsion about the N2–N3 axis, it was not feasible to perform a simple harmonic analysis and the associated calculation of the corresponding energy levels associated with that degree of freedom, in the way described in the previous section for the methyl rotation. The difficulties originate, firstly, from the fact that the two alkyl substituents at center N3 are not equivalent by symmetry. This result is in agreement with crystallographic data[15] and NMR work.[5] The consequence of this lack of symmetry is evident in Figures 2 and 4. The potential energy surface for internal rotation about the N2–N3 axis produces two minima, and two barriers differing considerably in their height. To account for this finding in a phenomenological way, eq 1 has to be modified by adding of a series of sine functions.[22] In the modified form, eq 1 reads

$$V(\tau) = \sum_{i=1}^{\infty}(V_i/2)(1-\cos(i\tau)) + \sum_{k=1}^{\infty}V_k^*(\sin(k\tau)) \qquad (5)$$

Two different strategies have been used in the least squares fitting procedure, to obtain the parameters of the potential energy curve

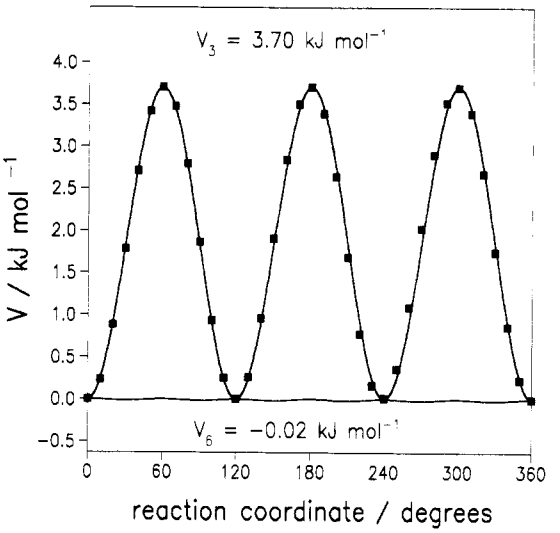

Figure 3. Potential energy curve for the internal rotation of methyl group C8 in compound **1**. This figure is a slice through the potential energy surface with the N1–N2–N3–C8 dihedral angle fixed at the minimum energy conformation; the PM3 parametrization was used in the calculation. Squares, calculated data points; solid line, 3-fold contribution to the rotational potential; dashed line, 6-fold term (eq 2).

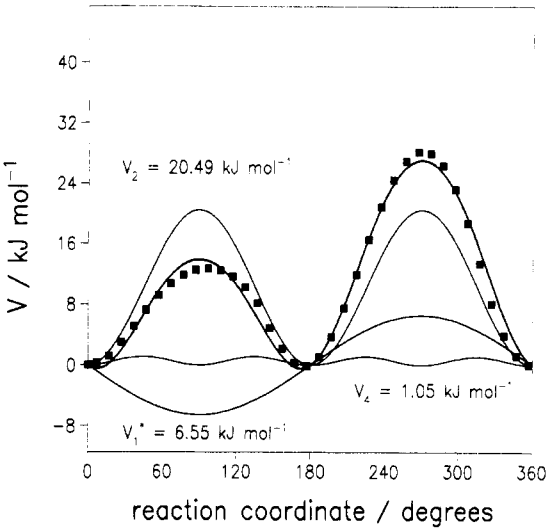

Figure 4. Potential energy curve for torsion around the N2–N3 axis in compound **1**. The figure is a slice through the potential energy surface calculated at the minimum of the methyl group torsional potential. Solid squares, energies calculated with the PM3 method; thin lines, contributions to the rotational potential obtained by least-squares analysis (three-parameter fit, as described in the text); bold line, overall potential according to eq 5.

for the motion about the N2–N3 axis. In a first attempt, four cosine and two sine terms were used in the least-squares fit, i.e., the six parameters V_1, V_2, V_3, V_4, V_1*, and V_2* were allowed to vary. Another fit to the calculated data was performed with a three parameter fit equation, in which only the terms containing V_2, V_4, and V_1* were retained. The accuracy of both fits was judged by inspection of the variance-covariance matrix.[23] The diagonal elements of this matrix, corresponding to the variance of the calculated parameters, reflect the deviations of the fitted data from the proposed model.

The results of both fits to the calculated potential energy data are are listed in Table 4, along with experimental barrier heights extracted from dynamic NMR measurements. NMR derived data for compounds **2** and **3** are taken from ref 5. The graphical representation of the three-parameter fit in Figure 4 demonstrates that the model is well capable of adequately representing the data.

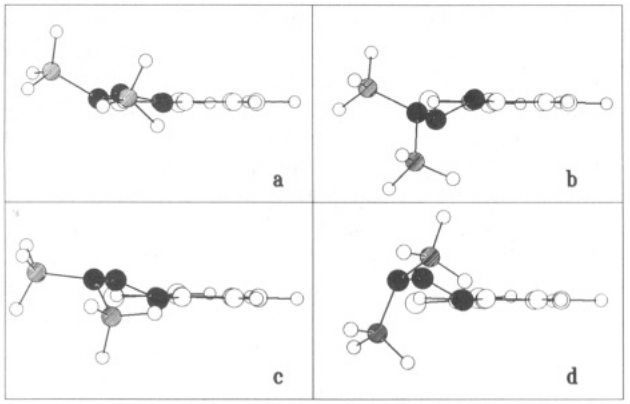

Figure 5. Molecular geometry of the triazene moiety at various stages of the internal motion around the N2 → N3 axis. Rotation is in the clockwise sense when viewed down this axis. The sequence shows the first minimum (a), the lower energy maximum (b), the second minimum (c), and the geometry at the second maximum (d). In each subfigure, the phenyl substituent is depicted in the same projection. Methyl group C atoms are hatched; nitrogen centers are represented by filled circles. Note the movement of the N2–N3 axis while the dihedral angle is varied from the values corresponding to the first energy maximum to the second energy minimum, and similarly from the second maximum back to the first minimum value. Selected structural parameters quantifying the accompanying changes in molecular geometry are given in Table 5.

TABLE 5: Change of Selected Parameters during the Internal Motion about the N2–N3 Axis in Compound 1 (cf. Figure 6)

parameter	Figure 6a	Figure 6b	Figure 6c	Figure 6d
N1–N2–N3–C9 dihedral angle	23.1	120.0	200.0	290.0
N1–N2 bond order	1.821	1.962	1.828	1.953
N2–N3 bond order	1.088	0.945	1.085	0.952
C1–N1–N2 bond angle	119.5	120.0	119.3	120.2
N1–N2–N3 bond angle	117.3	112.2	117.4	117.7
heat of formation/kJ mol^{-1}	–50.7	–38.0	–50.8	–22.6
ionization potential/eV	9.255	9.307	9.267	9.503

From the standard deviations of the estimated parameters (Table 4), it is evident that the three-parameter equation gives a better fit to the calculated data than the six-parameter model in the case of the AM1 computations. For the results of the PM3 parametrization, both models represent the calculated data with comparable accuracy; here the six-parameter equation yields somewhat smaller standard deviations than the three-parameter fit in the case of compounds **2** and **3**. This result appears reasonable as the torsional motion should be more complex with the ethyl- and isopropyl-substituted triazenes, as more atoms are involved.

Overviewing the results in Table 4, we notice that both described models provide a very satisfactory representation of the PM3 calculated data. In contrast, we observe that the variance–covariance matrix elements are rather large in case of the AM1 calculations. The reason for this difference will be analyzed in detail for compound **1**. From a close inspection of the potential energy (cf. Figure 2), one finds that the descent from the higher rotation barrier into the adjacent minimum of the surface is very steep. The energy drops by 40 kJ mol^{-1} as the relevant dihedral angle is increased from 140° to 150°. Additional calculations showed that the angular range of this steep energy decrease can be narrowed down further to the interval between 142° and 143°. This drop in potential energy is accompanied by a large travel of one of the methyl groups, which jumps from below the plane of the phenyl moiety to a position lying above that plane. The same behavior is observed if the direction of incrementing the dihedral angle is reversed, which shows that the result is not due to an accumulation of strain in the course of the grid calculation.

We note that the numerical agreement between calculated and experimental barrier heights is better for AM1, as compared to PM3 (cf. Table 4). However, the discontinuity of the potential energy curve obtained when using the AM1 parametrization raises the question whether the latter method is capable of providing a physically reasonable description of internal motion around the N2–N3 axis. A possible origin of the discontinuity may be the evidently bad description of electron density at the nitrogen center N3, as discussed above. As the mentioned anomaly is observed for the ethyl and isopropyl-substituted triazene compounds as well, only the results of the PM3 calculations will be discussed in the following paragraphs.

All compounds investigated show asymmetric internal rotor behavior regarding the N2–N3 degree of freedom. This property renders the computation of the corresponding eigenvalues quite difficult, and prevents the use of a harmonic oscillator approximation.[17] In the course of the analysis, it became evident that the motion modeled in our calculation is not a simple internal rotation, as mentioned before. This contrasts the methyl group internal rotation discussed above, which is adequately described as a relative reorientation of two rigid tops around a space fixed axis. In the case of motion around the N2–N3 axis, the two tops performing internal rotation are *not* connected by a space-fixed axis.

To illustrate the changes in geometry occurring during internal rotation, the molecular geometry of compound **1** is displayed in Figure 5 at four different values of the C9–N3–N2–N1 dihedral angle. The equilibrium geometry is shown in (a). At the first (lower) energy barrier, loss of conjugation between the lone pair at N3 and the aromatic π-electron system after a 90° internal rotation is evident (b). Figure 5c depicts the structure corresponding to the second minimum, whereas in (d) the geometry of the second (higher) maximum of the potential energy curve is presented. It should be noted that the phenyl moiety has been fixed in the same projection for all parts of Figure 5.

A set of electronic and geometrical parameters is listed in Table 5 to indicate the changes in molecular properties during internal motion. From the graphs the above statement that the internal motion about the N2–N3 axis is not a "pure" internal rotation becomes obvious. In particular, the *position* of the N2–N3 axis moves from below the phenyl ring at the first energy maximum (Figure 5b) to above the phenyl ring in the second energy minimum. This implies that the internal motion is composed of two processes, i.e., the rotation about the N2–N3 axis and the "crankshaft" motion of the N2–N3 axis itself. An additional explanation for the different heights of the maxima found in the potential energy surface is found on inspection of Table 5. The N1–N2–N3 bond angle at the first maximum is relaxed to 112.2°, whereas at the second maximum it remains close to the value obtained for the minima (117°).

Comparison with Experimental Data. To check the reliability of the calculations performed, IR and Raman spectra have been recorded for all of the compounds; results are presented in Figure 6. Assignments of measured frequencies to the vibrational modes have been made on the basis of a recent study of tetramethyltetrazene.[24] To establish the validity of this comparison, we have tested whether the electronic structure and the geometrical parameters calculated for this compound are similar to those of the triazene derivatives investigated in the present study. This was indeed found to be the case; for example, bond orders calculated under the PM3 model are 1.840 for the N=N bond, and 1.030 for the N–N bond in this compound. With the AM1 parametrization, the corresponding values were obtained as 1.764 and 1.050, respectively, in close similarity to the values given in Table 2. Furthermore, the calculated conformation at the methyl-substituted nitrogen centers of tetramethyltetrazene resembles the conformation at center N3 in our triazene compounds.

On the basis of this similarity, we are confident to follow the argumentation of ref 24 and assign the Raman bands at 192–194 cm^{-1} to the N2–N3 torsional mode; the signals in the 260–300

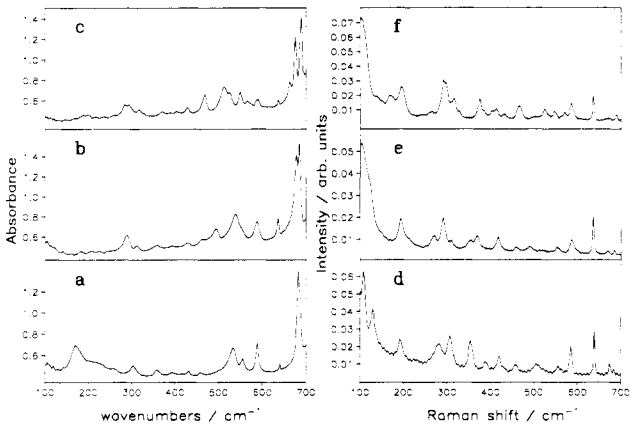

Figure 6. FT Raman and FTIR spectra of the triazene compounds, recorded with a resolution of 1 cm^{-1}. a, d: 1-(3-carboxyphenyl)-3,3-dimethyltriazene. b, e: 1-(3-carboxyphenyl)-3,3-diethyltriazene. c, f: 1-(3-carboxyphenyl)-3,3-diisopropyltriazene.

cm^{-1} range are attributed to methyl torsional vibrations. Further evidence for this assignment is given by the fact that the mentioned frequencies respond to changes in the N2–N3 bond order. This trend parallels the earlier observed correlation between the experimental free energy of internal rotation, $\Delta G^{\ddagger}$, and the N2–N3 bond order.[7] Furthermore, the complexity of the signal group at ~260–300 cm^{-1} increases when the alkyl substituents are changed from methyl to isopropyl groups. On the basis of this assignment, we find—as was already stated above—that calculated barrier heights are smaller than those observed experimentally for both degrees of freedom investigated.

First we wish to reemphasize that the calculated methyl group rotational frequencies are smaller than the experimental ones (cf. Table 3). With the geometrical parameters obtained within the PM3 model, we calculate a moment of inertia of 5.48×10^{-47} kg m^2 for the methyl group. Using this value, we may deduce the barrier height in the harmonic approximation from the spectroscopically obtained data. If the frequencies from the Raman spectrum are taken into account, we find experimental barrier heights of 20.7 and 24.5 kJ mol^{-1} for the two inequivalent methyl groups of compound **1**.

For the degree of freedom related to torsion about the N2–N3 axis, a similar estimate from the vibrational frequencies is not possible for the reasons discussed previously in the text. Therefore, a comparison is only made between experimentally deduced barrier heights from NMR, and the maximum barrier height calculated from the three parameter fit. Since the only terms contributing to total barrier height are $|V_2|$ and $|V_1^*|$, we find barrier heights of 27.0 (40.6) kJ mol^{-1} for the bis-methyl-substituted compound, 32.4 (40.9) kJ mol^{-1} for the bis-ethyl-substituted triazene, and 32.1 (43.1) kJ mol^{-1} for the bis-isopropyl-substituted compound, respectively. Numbers in parentheses refer to values obtained within the AM1 parametrization. These values are considerably smaller than the experimental results for either $\Delta G^{\ddagger}$ or the activation energy E_a. Plotting the calculated barrier heights against the corresponding experimental values, we observe that both parametrizations describe the experimentally observed *trends* in barrier height equally well (cf. Table 4; plots not shown). The correlation coefficient of linear regression for the data calculated using PM3 is 0.89, whereas the correlation coefficient under the AM1 model is 0.88.

Conclusions

A model for the shape of the potential energy function governing internal rotation about the N2–N3 axis in 1-aryl-3,3-dialkyltriazene compounds has been established. It accounts for the inequivalence of the alkyl substituents evidenced by NMR spectroscopy and crystallographic data and includes a "crankshaft" motion of the N2–N3 axis in addition to the overall rotation of the alkyl substituents. Infrared (FTIR and FT Raman) spectra were recorded in order to check the reliability of the calculations performed. Calculated barrier heights are too small as compared to experimentally derived data, for both parametrizations used.

The PM3 calculations provide a more adequate description of the *shape* of the potential energy function than those performed under the AM1 parametrization, although for the latter the calculated barrier values are closer to the values derived from NMR measurements. The difference in performance of the two parametrizations was traced back to the different description of partial charges in the triazene moiety. The PM3 model yields partial charges corresponding to a dipolar charge distribution within the triazeno groups, which is supported by a variety of chemical and spectroscopic evidence.

Acknowledgment. We are indebted to O. Nuyken and J. Stebani, who prepared the triazene compounds and made them available for the present study. Sincere thanks are due to H. Keppler for recording the FIR spectra, and to J. Reiner for the recording of the NMR spectra. The authors also wish to thank T. Clark for making the SCAMP 4.30 program available and for helpful discussions. Financial support of this work by grants of the Deutsche Forschungsgemeinschaft (SFB 213) and by the Verband der chemischen Industrie are gratefully acknowledged.

References and Notes

(1) Lippert, T.; Stebani, J.; Nuyken, O.; Wokaun, A.; Ihlemann, J. *Angew. Makromol. Chem.* **1993**, *213*, 127.
(2) Stasko, A.; Adamcik, V.; Lippert, T.; Wokaun, A.; Dauth, J.; Nuyken, O. *Makromol. Chem.* **1993**, *194*, 3385.
(3) Lippert, T.; Stebani, J.; Nuyken, O.; Stasko, A.; Wokaun, A. *J. Photochem. Photobiol. A* **1993**, *78*, 139.
(4) Akthar, M. H.; McDaniel, R. S.; Feser, M.; Oehlschlager, A. C. *Tetrahedron* **1968**, *24*, 3899.
(5) Lippert, T.; Wokaun, A.; Dauth, J.; Nuyken, O. *Magn. Res. Chem.* **1992**, *30*, 1178.
(6) Zimmermann, F.; Lippert, T.; Beyer, C.; Stebani, J.; Nuyken, O.; Wokaun, A. *Appl. Spectrosc.* **1993**, *47*, 986.
(7) Panitz, J.-C.; Lippert, T.; Stebani, J.; Nuyken, O.; Wokaun, A. *J. Phys. Chem.* **1993**, *97*, 5246.
(8) Ramos, M. N.; Pereira, S. R. *J. Chem. Soc., Perkin Trans. 2* **1986**, 131.
(9) Clark, T. Universität Erlangen, 1990.
(10) Stewart, J. J. P. MOPAC 4.0, QCPE Program 455.
(11) Liotard, D. A.; Healy, E. F.; Ruiz, J. M.; Dewar, M. J. S. AMPAC, QCPE Program 506.
(12) Herrmann, F.; Kerber, A.; Wokaun, A. SHOWMOLE, Universität Bayreuth, 1991.
(13) Dewar, M. J. S.; Zoebisch, E. G.; Healy, E. F.; Stewart, J. J. P. *J. Am. Chem. Soc.* **1985**, *107*, 3902.
(14) Stewart, J. J. P. *J. Comput. Chem.* **1989**, *10*, 209, 221. Stewart, J. J. P. *J. Comput. Aid. Mol. Design* **1990**, *4*, 1.
(15) Fronczek, F. R.; Hansch, C.; Watkins, S. F.; *Acta Crystallogr. C* **1988**, *44*, 1651.
(16) Stewart, J. J. P. In *Reviews in Computational Chemistry*; Lipkowitz, K. B., Boyd, D. B., Eds.; VCH Publishers: New York, 1990; Vol. 1, pp 45–81.
(17) Lister, D. G.; Macdonald, J. N.; Owen, N. L. *Internal Rotation and Inversion*; Academic Press: London, 1978.
(18) Press, W. *Single-Particle Rotations in Molecular Crystals*; *Springer Tracts in Modern Physics*; Springer: Berlin, 1981; Vol. 92.
(19) Panitz, J.-C.; Diplomarbeit, Technische Hochschule Darmstadt, 1991.
(20) Herzberg, G. *Infrared and Raman Spectra of Polyatomic Molecules*; Van Nostrand: New York, 1945; pp 225–227.
(21) Fabian, W. M. F. *J. Comput. Chem.* **1988**, *9*, 369.
(22) Radom, L.; Hehre, W. J.; Pople, J. A. *J. Am. Chem. Soc.* **1972**, *94*, 2371.
(23) Massart, D. L.; Vanderginste, B. G. M.; Deming, S. N.; Michotte, Y.; Kaufman, L. *Chemometrics: A Textbook*; Elsevier: Amsterdam, 1988.
(24) Harris, W. C.; Knight, L. B., Jr.; MacNamee, R. W.; Durig, J. R. *Inorg. Chem.* **1974**, *13*, 2297.